

ON THE QAM PARALLEL TURBO-TCM SCHEMES USING RECURSIVE CONVOLUTIONAL $GF(2^N)$ ENCODERS

Adrian Florin Păun¹, Călin Vlădeanu¹, Ion Marghescu¹, Safwan El Assad², and Alexandru Marțian¹

¹Telecommunications Department, University Politehnica of Bucharest

1-3 Iuliu Maniu Bvd., Zip 061071, Bucharest, Romania

phone: + (40) 21 402 4765, fax: + (40) 21 402 4765, email: {adi, martian}@radio.pub.ro, {calin, marion}@comm.pub.ro

²IREENA, École Polytechnique de l'Université de Nantes

Rue Christian Pauc, B.P. 50609, 44306 Nantes, cedex 3, France

phone: + (33) 2 40 68 30 36, fax: + (33) 2 40 68 32 32, e-mail: safwan.elassad@univ-nantes.fr

ABSTRACT

In this paper, parallel turbo quadrature amplitude modulation – trellis coded modulation (Turbo QAM-TCM) schemes are designed using recursive convolutional encoders over Galois field $GF(2^N)$. These encoders are designed using the nonlinear left-circulate (LCIRC) function. The LCIRC function performs a bit left circulation over the representation word. An optimum 1-delay $GF(2^N)$ recursive convolutional encoder scheme using LCIRC (RC-LCIRC) is proposed for QAM-TCM schemes. The minimum Euclidian distance is estimated for these QAM-TCM schemes and it is shown that these structures offer the maximum coding gains. However, the RC-LCIRC encoders are less complex than the corresponding binary encoders are. The optimum RC-LCIRC encoder is used as component encoder of a parallel turbo QAM-TCM transmission scheme, using the iterative multi-level log-MAP algorithm in the receiver. The bit error rate (BER) is estimated by simulation for the proposed Turbo QAM-TCM transmissions over an additive white Gaussian noise (AWGN) channel, and the results are similar to the conventional Turbo-TCM schemes.

1. INTRODUCTION

The nonlinear functions were used lately in several blocks of communications systems to increase their performances.

Frey [1] proposed a chaotic digital infinite impulse response (IIR) filter for a secure communications system. The Frey filter contains a nonlinear function named left-circulate function (LCIRC), which provides the chaotic properties of the filter. This work considered the Frey encoder as a digital filter, operating over Galois field $GF(2^N)$.

Barbulescu and Guidi [2] made one of the first attempts regarding the possible use of the Frey encoder in a turbo-coded communication system, but the paper lacks of proof for the stated performance enhancement.

In [3] it was demonstrated that the Frey encoder with finite precision (wordlength of N bits) presented in [1] is a recursive convolutional encoder operating over $GF(2^N)$. New

methods for enhancing the performances of the PAM – trellis-coded modulation (PAM-TCM) and the phase shift keying – trellis-coded modulation (PSK-TCM) transmissions over a noisy channel were proposed in [4] and [5], respectively. These encoders follow the rules proposed by Ungerboeck [6] for defining optimum trellis-coded modulations by proper set partitioning. Two-dimensional (2D) TCM schemes using a different trellis optimization method for Frey encoder were proposed in [7].

The turbo coding scheme introduced by Berrou and Glavieux in their seminal paper [8] allow communications systems performances close to the Shannon limit, by concatenating in parallel recursive convolutional encoders in the transmitter and using iterative decoding algorithms in the receiver. Turbo schemes were developed as well for the TCM schemes [9], [10], [12].

In the present work, the recursive convolutional LCIRC (RC-LCIRC) from [5] is adapted to and introduced in a parallel turbo quadrature amplitude modulation QAM-TCM transmission scheme, and the performances of this scheme are analyzed in case of transmitting over a channel with additive white Gaussian noise (AWGN). A similar analysis was performed in [11] for the turbo PSK-TCM transmission scheme.

The paper is organized as follows. Section 2 is presenting the RC-LCIRC encoder operating over Galois field $GF(2^N)$ and its use for optimum PSK-TCM schemes. The asymptotic gain of rate $(N-1)/N$ RC-LCIRC encoder is estimated. In Section 3, a parallel turbo QAM-TCM transmission scheme using RC-LCIRC component encoders is proposed. A multilevel log-MAP algorithm is used for the iterative detection. The simulated bit error rate (BER) performance in an AWGN channel is plotted in Section 4 for the 16 QAM-TCM transmission as compared to 8PSK, using two types of mappings: Gray and set partitioning (SP). The coding gains of 16QAM-TCM schemes using these different mappings, as compared to the uncoded modulation and the non-iterative schemes, are derived from simulations. Finally, the conclusions are drawn and some perspectives are presented in Section 5.

This work was supported in part by the Romanian UEFISCSU PN-2 Project 116/01.10.2007, and by the French ANR Project ASCOM.

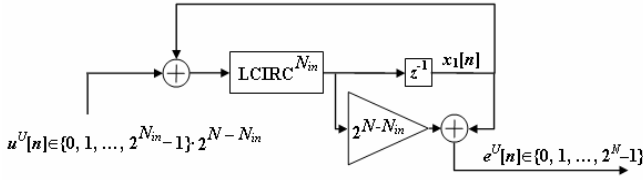


Figure 1. – Rate N_{in}/N optimum $GF(2^N)$ recursive convolutional LCIRC encoder for N_{in} b/s/Hz.

2. OPTIMUM RECURSIVE CONVOLUTIONAL LCIRC ENCODERS FOR PSK-TCM SCHEMES

In this section, a new family of recursive convolutional encoders operating over Galois field $GF(2^N)$ and their use for optimum QAM-TCM schemes are presented.

The main component of the chaotic encoder introduced by Frey in [1] and the recursive convolutional encoder presented in [3] is the nonlinear LCIRC function. Let us denote by N the wordlength used for binary representation of each sample. The LCIRC function is used as a typical basic accumulator operation in microprocessors and performs a bit rotation by placing the most significant bit to the less significant bit, and shifting the other $N-1$ bits one position to a higher significance.

The block scheme for an optimum recursive convolutional LCIRC (RC-LCIRC) encoder, using one delay element and the LCIRC function is presented in Fig. 1 [5]. For each moment n , $u[n]$ represents the input data sample, $x_1[n]$ denotes the delay output or the encoder current state, and $e[n]$ is the output sample. The superscript U denotes that all the samples are represented in unsigned N bits wordlength, i.e., $u^U[n], e^U[n] \in [0, 2^N-1]$. The encoding rate for the encoder in Fig. 1 is the ratio between the input wordlength N_{in} and the output wordlength $N=N_{out}$, i.e., $R=N_{in}/N$ [7], [8]. $LCIRC^{N_{in}}$ represents the LCIRC function application for N_{in} times consecutively. Both adders and the multiplier are modulo- 2^N operators.

For a fixed output wordlength N , an optimum recursive convolutional encoder can be designed for each input wordlength $N_{in} \in \{1, 2, \dots, N-1\}$, for which the encoding rate is $R = \{1/N, 2/N, \dots, (N-1)/N\}$ [4], [5].

The trellis complexity of the codes generated with the scheme in Fig. 1 increases with the wordlength, because the number of trellis states grows exponentially with the output wordlength, i.e., 2^{2N} , while the number of transitions originating from and ending in the same state grows exponentially with the input wordlength, i.e., $2^{2N_{in}}$.

It can be easily demonstrated that the minimum Euclidian distance for the PSK-TCM scheme using encoder in Fig. 1 has the following expression [5]:

$$d_{E, R=N_{in}/N, 2^N-PSK}^2 = \begin{cases} 2(\Delta_{2^{N-N_{in}-1}})^2 + \sum_{i=0}^{2^{N-N_{in}}-2} (\Delta_i)^2, & \text{for } N_{in} \in \left\{1, \dots, \frac{N}{2}-1, \frac{N}{2}+1, \dots, N-1\right\} \\ 2(\Delta_{2^{N-N_{in}-1}})^2 + (\Delta_0)^2, & \text{for } N_{in} = \frac{N}{2} \end{cases} \quad (1)$$

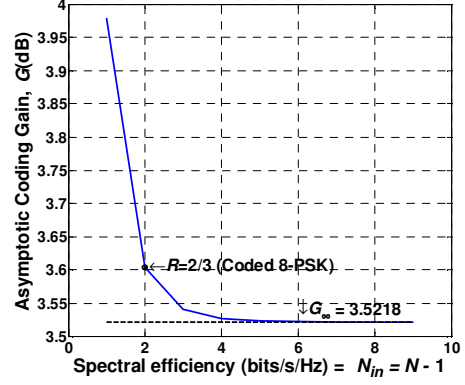


Figure 2. – Asymptotic gain as function of the spectral efficiency for rate $(N-1)/N$ optimum $GF(2^N)$ recursive convolutional LCIRC encoders.

where Δ_k represents the k th order Euclidian distance between the M -PSK signal constellation points. We can write the following expressions of the M -PSK Euclidian distances in the ascending order:

$$\Delta_k = 2 \cdot \sin[(k+1) \cdot \pi / M], k \in \{0, 1, \dots, \log_2(M)-1\} \quad (2)$$

For example, let us consider the optimum encoders for the 8-PSK-TCM scheme, i.e., the output wordlength equal to 3, i.e., $N=3$. The input wordlength may take three values $N_{in} \in \{1, 2\}$, and the corresponding encoding rates are $R \in \{1/3, 2/3\}$. For the rate 1/3 encoder the scheme in Fig. 1 is set with all the values corresponding to $N_{in}=1$. From (1) and (2) results that the minimum distance of this code is $d_{E, R=1/3, \text{opt.}, 8\text{-PSK}, u^U \in \{0,4\}}^2 = 14$, having a coding gain of $10 \cdot \log_{10}(d_{E, R=1/3, \text{opt.}, 8\text{-PSK}, u^U \in \{0,4\}}^2 / d_{E, R=1, N=3, \text{opt.}, 8\text{-PSK}}^2) = 10 \cdot \log_{10}(14/1.1716) \approx 10.77$ dB over the optimum 8PSK ($N=3$) using a rate 1 encoder. For the rate 2/3 encoder ($N_{in}=2$) the minimum distance of this code is $d_{E, R=2/3, \text{opt.}, 8\text{-PSK}, u^U \in \{0,2,4,6\}}^2 = 4 + 4 \cdot \sin^2(\pi/8) \approx 4.5858$, having a coding gain of approximately 5.93 dB over the optimum 8PSK ($N=3$) using a rate 1 encoder. The rate 1 optimum encoder is obtained for $N_{in} = N$, for any value of N , considering that $LCIRC^0(x^U) = LCIRC^N(x^U) = x^U$ assumes no bit circulation. This rate 1 optimum encoder offers a minimum distance of $d_{E, R=1, \text{opt.}, N=3, \text{opt.}, 8\text{-PSK}}^2 = 8 \cdot \sin^2(\pi/8) \approx 1.1716$.

It can be easily demonstrated starting from (1) that all the rate $(N-1)/N$, for any N value, the optimum recursive convolutional LCIRC encoders are offering the same minimum distance as the corresponding binary optimum encoders determined by Ungerboeck in [6]. For example, the above-mentioned rate 2/3 encoder ($N_{in}=2$) has the minimum Euclidian distance of 4.5858 determining an asymptotic coding gain of 3.6 dB. Using the expressions in (1) we can easily plot the asymptotic gain of optimum rate $(N-1)/N$ LCIRC as a function of the spectral efficiency $N-1$. The results are presented in Fig. 2.

The asymptotic coding gain is estimated using the following expression:

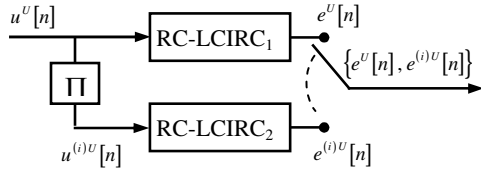


Figure 3. – Turbo TCM encoder with RC-LCIRC.

$$G[dB] = 10 \cdot \log_{10} \left(\frac{d_{E, R=(N-1)/N, 2^N\text{-PSK}}^2}{\Delta_{0, 2^{(N-1)}\text{-PSK}}} \right) \quad (3)$$

where $d_{E, R=(N-1)/N, 2^N\text{-PSK}}^2$ denotes the minimum Euclidian distance of the rate $(N-1)/N$ LCIRC TCM scheme using a PSK modulation with 2^N phase levels, and $\Delta_{0, 2^{(N-1)}\text{-PSK}}$ represents the minimum Euclidian distance in the $2^{(N-1)}$ -PSK non-coded signal constellation. Hence, the asymptotic coded gain specifies the gain of the coded scheme when doubling the signal constellation size over the non-coded signal. As shown in Fig. 2 the asymptotic gain decays rapidly to a limit value when the number of signal levels increases. Similar results can be obtained for QAM-TCM schemes.

However, the $\text{GF}(2^N)$ optimum recursive convolutional LCIRC encoders are less complex than the corresponding binary encoders. The memory size of the binary encoders increases logarithmically with the number of states in the trellis, while the $\text{GF}(2^N)$ optimum recursive convolutional LCIRC encoders include only one delay element, no matter what the trellis complexity is. As another advantage of these encoders, we can also mention the Euclidian distance compact expression as a function of N_{in} and N .

3. RC-LCIRC ENCODER IN QAM TURBO-TCM SCHEME

Fig. 3 shows the turbo TCM encoder for 2^N -QAM modulation. The information sequence and the N_{in} bits block-wise interleaved sequence are fed into component encoders RC-LCIRC₁ and RC-LCIRC₂ of rate N_{in}/N , and mapped into 2^N -QAM symbol sequences (x_n). The non-systematic nature of RC-LCIRC encoder does not permit the parity bits puncturing as in traditional turbo-TCM schemes. Hence, the overall coding rate for the scheme in Fig. 3 is $N_{in}/(2 \cdot N)$. The 2^N -QAM symbol sequence is transmitted over a noisy channel. The received signal over the n -th symbol interval is given by:

$$y_n = x_n + w_n \quad (4)$$

where w_n is an additive white gaussian noise (AWGN) sequence and x_n denotes the 2^N -QAM symbol sequence mapped from the encoder output sequence $\{e^u[n], e^{(i)u}[n]\}$.

The receiver structure, shown in Fig. 4, has two components that use multilevel version of log-MAP algorithm. The odd symbols from the received sequence are fed into first component decoder that corresponds to the RC-LCIRC₁ in order to compute the a posteriori log likelihood ratio (LLR) per transmitted bit L_{ap} , as following:

$$L_{ap}(b_m | \mathbf{y}) = \ln \frac{P(b_m = 1 | \mathbf{y})}{P(b_m = 0 | \mathbf{y})} \quad (5)$$

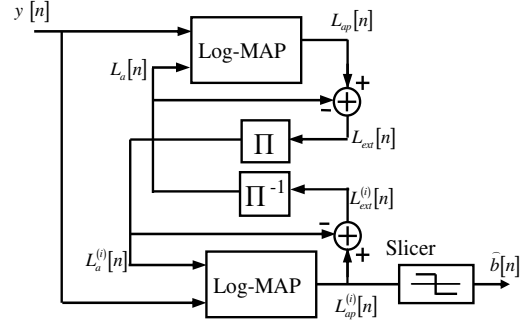


Figure 4. – Iterative turbo-TCM receiver.

where b_m is the t -th bit from n -th encoder input information word, $\{\mathbf{b}_n\} \leftrightarrow u^U$ with $t=1 \dots 2^{N_{in}}$, and \mathbf{y} is the received symbol vector.

Using Bayes' theorem under the assumption of statistically independent bits, the joint probabilities can be split into products:

$$L_{ap}(b_m | \mathbf{y}) = \ln \frac{\sum_{b_m \in \mathbf{b}_t^{(1)}} p(\mathbf{y} | x_n) \cdot P(x_n | \mathbf{b}_t^{(1)}) \cdot \prod_{t=1}^{N_{in}} P(b_m = 1)}{\sum_{b_m \in \mathbf{b}_t^{(0)}} p(\mathbf{y} | x_n) \cdot P(x_n | \mathbf{b}_t^{(0)}) \cdot \prod_{t=1}^{N_{in}} P(b_m = 0)} \quad (6)$$

where $\mathbf{b}_t^{(0)}$ and $\mathbf{b}_t^{(1)}$ are the sets of $2^{N_{in}-1}$ words of input bits with the t -th position bit $b_t = 0$ or $b_t = 1$, respectively. The third term in (6) represents the a priori bit knowledge fed by the other decoder $L_a(b_m)$. The first two terms in both sums from denominator and nominator of (6) represent the symbol probability that depends on a priori bit values and trellis encoder constraints, which are used in transition metric computation of multilevel log-MAP algorithm [9]. The relation (6) is evaluated iteratively as:

$$L_{ap}(b_m | \mathbf{y}) = \max_{b_m \in \mathbf{b}_t^{(1)}}^* \left(p(\mathbf{y} | x_n) \cdot P(x_n | \mathbf{b}_t^{(1)}) \cdot \prod_{t=1}^{N_{in}} P(b_m = 1) \right) - \max_{b_m \in \mathbf{b}_t^{(0)}}^* \left(p(\mathbf{y} | x_n) \cdot P(x_n | \mathbf{b}_t^{(0)}) \cdot \prod_{t=1}^{N_{in}} P(b_m = 0) \right) \quad (7)$$

using an eight entries approximation table of the so called Jacobian Logarithm, given by [9]:

$$\max^*(a, b) = \ln(e^a + e^b) = \max(a, b) + \ln(1 + e^{-|a-b|}) \quad (8)$$

Then, the extrinsic information L_{ext} is calculated by subtracting the a priori LLR $L_a(b_m)$ from $L_{ap}(b_m)$. The extrinsic information shows the increment of the decoded symbol reliability. The extrinsic information sequence from the first log-MAP decoder (corresponding to the component encoder RC-LCIRC₁) is interleaved and fed into the second component decoder as a priori value, $L_a^{(i)}$. It corresponds to the component encoder RC-LCIRC₂. At the same time, the even order received symbols sequence is also fed into the second decoder and then this decoder calculates the extrinsic information, $L_{ap}^{(i)}$. This extrinsic information sequence is deinterleaved and fed back into the first component decoder as a priori value, L_a , thus ending each iteration.

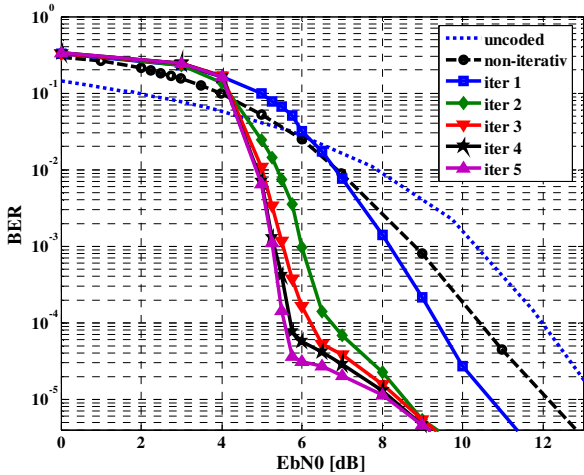


Figure 5. – BER for 16QAM turbo-TCM with Gray mapping.

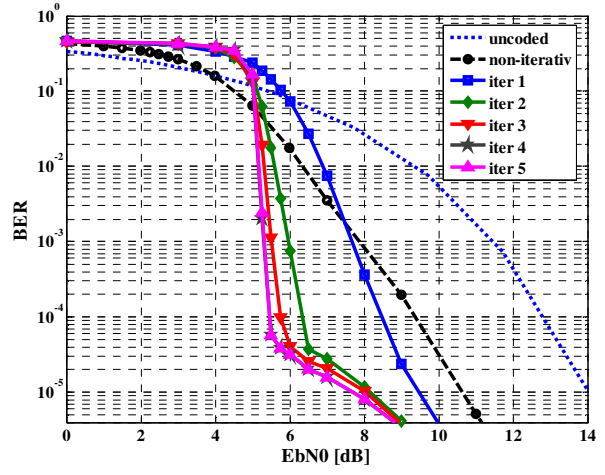


Figure 6. – BER for 16QAM turbo-TCM with anti-Gray mapping.

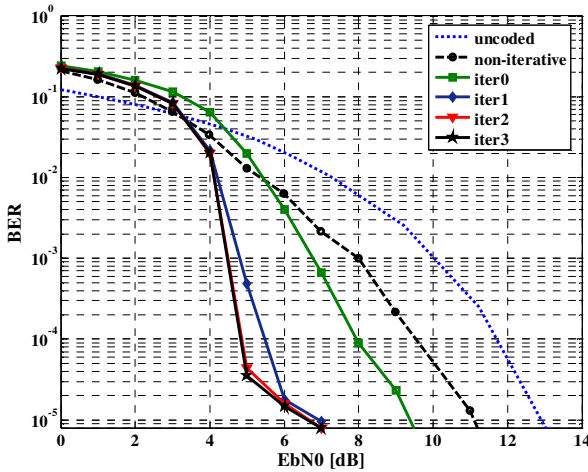


Figure 7. – BER for 8PSK turbo-TCM with Gray mapping.

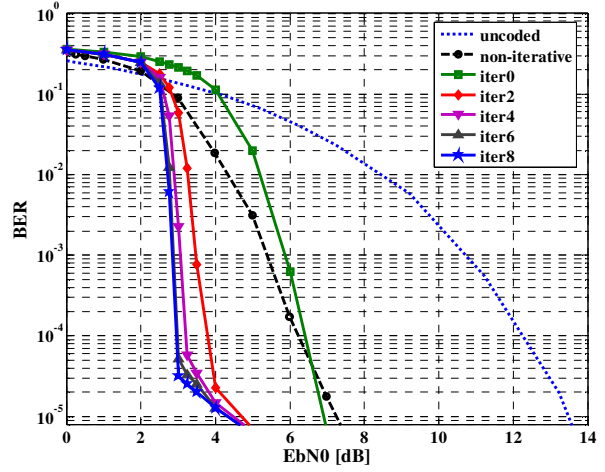


Figure 8. – BER for 8PSK turbo-TCM with anti-Gray mapping.

The role of deinterleaver is to rearrange the sequence of extrinsic information in the order corresponding to the received information from the first decoder component input. At the last iteration, a final decoded bit is obtained from the sign of L_{ap} .

4. SIMULATION RESULTS

The turbo-TCM scheme proposed in Section 3 was tested for 8-PSK and 16-QAM modulation by simulation over an AWGN channel, using an equivalent symbol wise block interleaver of length 31×31 . Both component encoders in the turbo-TCM scheme in Fig. 3 are identical rate-2/3 RC-LCIRC encoders for 8-PSK and rate-3/4 for 16-QAM, respectively. Hence, the overall coding rate is 1/3 for 8-PSK modulation and 3/8 for 16-QAM modulation, respectively. The TCM employed the modulations 8-PSK and 16-QAM with two mapping rules: Gray, and anti-Gray, where symbols at minimum Euclidean distance differ in one bit or in maximum number of bits, respectively [12].

Each of following simulation results are shown as BER performances versus E_b/N_0 , where E_b is the signal energy per one information bit and N_0 is one-sided power spectral density of the background noise.

Figure 5 shows the bit error rate (BER) performances of turbo-TCM using 16-QAM, Gray labeling. At 5-th iteration, we observe a 7 dB gain as compared with non coding scheme, for $BER=4 \cdot 10^{-5}$.

This scheme provides a 5.5dB gain over non-iterative scheme and 4 dB improvement through five iterations.

In figure 6 the BER performances of 16-QAM, anti-Gray labeling over first five iterations are depicted. Further iteration do not improve decoder/detector performances. This scheme offers about 8 dB gain versus encoded 16-QAM modulation and 4.25 dB gain as compared with non-iterative scheme.

Figure 7 shows the BER performances using 8-PSK, Gray labeling over first three iterations. Further iteration do not improve decoder/detector performances. This scheme offers about 8 dB gain versus encoded 8-PSK modulation and 2 dB as compared with non-iterative scheme.

BER performances for 8-PSK, anti-Gray labeling is shown in figure 8. This scheme attained the best threshold from all three mapping rules. It needs 3dB and 8 iterations to perform at $BER=3 \cdot 10^{-5}$. It provides 10dB gain versus uncoded modulation and 3.7dB as compared with non-iterative scheme.

The increased throughput of 16-QAM modulation has a penalty of 1dB and 2 dB for Gray and anti-Gray mapping respectively, compared to 8-PSK modulation.

We can note that the BER floor is about 10^{-5} for all simulations. This is due to low constraint length of the block interleaver, i.e., 961 symbols, and is relatively independent of the modulation type and mapping rule.

5. CONCLUSIONS

It was shown that the proposed RC-LCIRC encoder can be used as a component encoder in turbo-TCM schemes. The BER performances improvement with iterations was demonstrated by means of simulations. For simulations, we considered the 16-QAM and 8-PSK turbo-TCM scheme, using two mappings: Gray and anti-Gray. Similar to the classical turbo-TCM scheme, the maximum coding gain is determined for the anti-Gray mapping. Nevertheless, the nonlinear LCIRC function drives to low complexity encoder, while the lack of non-systematic property attains good performances in iterative schemes.

In further studies it is necessary to evaluate the performances using EXIT chart and investigate the punctured version of this turbo-TCM schemes. In addition, the scheme performances analysis when transmitting over a channel with fading requires further attention.

REFERENCES

- [1] D. R. Frey, "Chaotic digital encoding: An approach to secure communication," *IEEE Trans. Circuits and Systems – II: Analog and Digital Signal Processing*, vol. 40, pp. 660–666, October 1993.
- [2] S. A. Barbulescu, A. Guidi, and S. S. Pietrobon, "Chaotic turbo codes," *Proc. IEEE Int. Symp. Inf. Theory*, Sorrento, Italy, June 25-30, 2000, pp. 123.
- [3] C. Vlădeanu, S. El Assad, J.-C. Carlach, and R. Quéré, "Improved Frey Chaotic Digital Encoder for Trellis-Coded Modulation," *IEEE Trans. Circuits and Systems – II*, vol. 56, no. 6, pp. 509-513, June 2009.
- [4] C. Vlădeanu, S. El Assad, J.-C. Carlach, R. Quéré, and I. Marghescu, "Optimum PAM-TCM Schemes Using Left-Circulate Function over $GF(2^N)$," *Proc. IEEE 9th Int. Symp. on Signals, Circuits and Systems - ISSCS 2009*, Iași, Romania, July 9-10, 2009, pp. 267-270.
- [5] C. Vlădeanu, S. El Assad, J.-C. Carlach, R. Quéré, and I. Marghescu, "Optimum $GF(2^N)$ Encoders Using Left-Circulate Function for PSK-TCM Schemes," *Proc. 17th European Signal Proc. Conf. - EUSIPCO 2009*, Glasgow, Scotland, Aug. 2009, pp. 1171-1175.
- [6] G. Ungerboeck, "Channel coding with multilevel/phase signals," *IEEE Trans. Information Theory*, vol. IT-28, no. 1, pp. 55-67, January 1982.
- [7] C. Vlădeanu, S. El Assad, J.-C. Carlach, R. Quéré, and C. Paleologu, "Chaotic Digital Encoding for 2D Trellis-Coded Modulation," *Proc. IEEE 5th Advanced Int. Conf. on Telecomm. - AICT 2009*, Venice, Italy, May 24-28, 2009, pp. 152-157.
- [8] C. Berrou and A. Glavieux, "Near optimum error correcting coding and decoding: turbo-codes," *IEEE Trans. on Comm.*, vol 44, no. 10, pp. 1261-1271, Oct. 1996.
- [9] H. Ogiwara, "Performance evaluation of parallel concatenated turbo trellis coded modulation," *IEICE Trans. Fundamentals*, pp. 2410-2417, Oct. 2001.
- [10] P. Robertson, T. Worz, "A novel bandwidth efficient coding scheme employing turbo codes"; *IEEE Conf. on Communications ICC 96*, June 1996, pp. 962 – 967.
- [11] C. Vlădeanu, A. F. Păun, S. El Assad, J.-C. Carlach, R. Quéré, and C. Paleologu, "New Recursive Convolutional $GF(2^N)$ Encoders for Parallel Turbo-TCM Schemes," accepted to *IEEE 6th Advanced Int. Conf. on Telecomm. - AICT 2010*, Barcelona, Spain, May 9-15, 2010.
- [12] F. Schreckenbach, N. Gortz, J. Hagenauer, and G. Bauch, "Optimized Symbol Mappings for Bit-Interleaved Coded Modulation with Iterative Decoding" , *IEEE Conf. Globecom '03*, 2003, pp. 3316 – 3320.